The DOI for this manuscript is doi: 10.1175/BAMS-D-16-0192.1

Hosannah, N., J. Gonzalez, R. Rodriguez-Solis, H. Parsiani, F. Moshary, L. Aponte, R. Armstrong, E. Harmsen, P. Ramamurthy, M. Angeles, L. León, N. Ramírez, D. Niyogi, and R. Bornstein, 2017: The Convection, Aerosol, and Synoptic-Effects in the Tropics (CAST) Experiment: Building an Understanding of Multi-Scale Impacts on Caribbean Weather via Field Campaigns. Bull. Amer. Meteor. Soc. doi:10.1175/BAMS-D-16-0192.1, in press.

The Convection, Aerosol, and Synoptic-Effects in the Tropics (CAST) Experiment: Building an Understanding of Multi-Scale Impacts on Caribbean Weather via Field Campaigns

[1]N. Hosannah, [1]J. González, [2]R. Rodriguez-Solis, [2]H. Parsiani, [1]F. Moshary, [2]L. Aponte, [2]R. Armstrong, [2]E. Harmsen, [1]P. Ramamurthy, [1]M. Angeles, [2]L. León, [2]N. Ramírez, [3]D. Niyogi, and [4]B. Bornstein

[1]The City College of New York, New York, NY

[2]University of Puerto Rico at Mayaguez, Mayaguez, PR

[3]Purdue University, West Lafayette, IN

[4]San Jose State University, San Jose, CA

Corresponding Author Address: Nathan Hosannah, NOAA CREST and Department of Mechanical Engineering, The City College of New York, New York, NY 10031

Email: nhosannah@gmail.com

Abstract

Modulated by global, continental, regional, and local scale processes, convective precipitation in coastal tropical regions is paramount in maintaining the ecological balance and socioeconomic health within them. The western coast of the Caribbean island of Puerto Rico is ideal for observing local convective dynamics as interactions between complex processes involving orography, surface heating, land cover, and sea-breeze trade-wind convergence influence different rainfall climatologies across the island. A multi-season observational effort entitled the Convection, Aerosol, and Synoptic-Effects in the Tropics (CAST) experiment was undertaken using Puerto Rico as a test case, to improve the understanding of island-scale processes and their effects on precipitation. Puerto Rico has a wide network of observational instruments, including ground weather stations, soil moisture sensors, a Next Generation Radar (NEXRAD), twice-daily radiosonde launches, and Aerosol Robotic Network (AERONET) sunphotometers. To achieve the goals of CAST, researchers from multiple institutions supplemented existing observational networks with additional radiosonde launches, three high resolution radars, continuous ceilometer monitoring, and air sampling in western Puerto Rico to monitor convective precipitation events. Observations during three CAST measurement phases (22 June–10 July 2015, 6–22 February 2016, and 24 April–7 May 2016) captured the most extreme drought in recent history (summer 2015), in addition to anomalously wet early rainfall and dry season (2016) phases. This short article presents an overview of CAST along with selected campaign data.

Caribbean rainfall modes

The Caribbean basin (85-60W, 8-22N) is a complex region in which understanding of the factors affecting water availability and associated rainfall production is important for the survival of millions of people and for the protection of sensitive ecosystems. Precipitation in the Caribbean is bimodal, with average peaks in the early (April to July) and late (August to November) rainfall seasons (averages of 216 and 178 mm month^{-1}, respectively), while June to July is a drier period within the early rainfall season (average of 114 mm month^{-1}) known as the midsummer drought. The dry season spans from December to March, and generally exhibits lower rainfall totals (averages between 12 and 60 mm month^{-1}).

Large-scale phenomena such as the ENSO and the North Atlantic Oscillation (with its associated North Atlantic High Pressure) modify sea surface temperatures (SSTs) and precipitable water in the Caribbean. SSTs are coupled with winds via changes in atmospheric stability that accompanies ENSO and NAO variations, and increases in water temperatures enhance air buoyancy, reducing vertical wind shear and promoting thermal convection. These wind-evaporation-SST feedbacks work down to local island scales to govern spatio-temporal moisture and rainfall patterns. An additional impactful element is the Saharan dust which transports across the Atlantic Ocean via the trade–winds in a dry air layer originating in North Africa. The dust transport is observed mostly during the summer months, with dust event intensity and frequency peaking in July. Dust events affect weather through their association with dry, warm air masses, and also by impacting cloud-scale microphysical processes via the suppression of cloud droplet growth mechanisms.

Although large-scale phenomena regulate spatio-temporal precipitation patterns in the Caribbean, the region's island-scale rainfall is also influenced by local convective processes modified by topography, land cover, soil moisture, and proximity to coastal waters. For example, the Puerto Rican Cordillera Central is a large east–west oriented mountain range along its central axis, with several peaks above 1 km (Fig. 1), the highest of which is Cerro de Punta at 1.34 km; the El Yunque natural rain forest is on the slopes of the highest peak on the eastern side of the island, at 1.07 km. These elevated sites induce orographic precipitation when moist air is forced upwards over them. Another location-dependent process occurs at the western edge of the island where the easterly trade-winds converge with westerly sea-breeze caused by surface heating, inducing or intensifying afternoon convective storms. These processes are further modified by changes in land cover and soil moisture, which impact sensible and latent heat fluxes.

To better understand how island-scale processes contribute to regional scale Caribbean precipitation, improved monitoring in the Caribbean islands must be considered. Currently, observational sensors are too few for in-depth analyses of island-scale rainfall patterns, as well as of local surface and atmospheric conditions. One exception is Puerto Rico with its extensive network of ground-based and in-situ sensors.

Gaps in the Puerto Rico observational network

Puerto Rico has over 40 active U.S. Geological Survey surface stations that measure precipitation, eight Natural Resource Conservation Service (NRCS) soil moisture sensor sites, a next generation radar (NEXRAD), three aerosol robotic network (AERONET) sunphotometers, and twice daily National Weather Service (NWS) radiosonde launches at 00 (20) and 12 (08) UTC (AST, Atlantic Standard Time). Since most of these instruments are located on, or deployed from the eastern side of the island, additional ground and in-situ sensors are necessary to properly monitor convective storm dynamics on the western side. The necessity to improve observational capabilities and to better understand local convective processes using western led to the Convection, Aerosol, and Synoptic-Effects in the Tropics (CAST) campaign.

CAST instrumentation and protocols

CAST was conducted by researchers (Fig. 2) from multiple institutions including the: University of Puerto Rico at Mayaguez (UPRM), City College of New York (CCNY), NWS in San Juan, Purdue University (PU), and San Jose State University (SJSU). Three CAST phases were scheduled to monitor atmospheric conditions in western Puerto Rico during three of its distinct seasons including the midsummer drought (Phase I: 22 June–10 July 2015), the dry season (Phase II: 6–22 February 2016), and the early rainfall season (Phase III: 24 April–7 May 2016). A phase summary is shown in Table 1.

Supplemental CAST instrumentation included up to twice-daily radiosonde launches, three high resolution radars, a ceilometer, a disdrometer, soil moisture sensors, and an aerosol speciation sampler, all on the west side of the island. Instrumented locations (Fig. 1) included UPRM (67.14W, 18.21N), fitted with a CL51 ceilometer (Vaisala), a CIMEL Electronique 318A spectral radiometer (AERONET), a disdrometer, and nearby Echo EC-5 soil moisture sensors at multiple depths (0.05, 0.1, 0.2, 0.5, and 1 m). These soil moisture sensors were placed at the same latitude (18.15N) as two western NRCS sites (Maricao 67W, 18.15N and Guilarte 66.77W, 18.15N) for comparative purposes. The disdrometer, soil moisture sensors, and ceilometer ran continuously. M10 radiosondes (Meteomodem) were launched from the roof of one of the UPRM buildings. The La Parguera (67.04W, 17.98N) site had an AERONET radiometer and an air sampler. Each of the three short-range dual polarized X-band Doppler radars at Cabo Rojo (67.18W, 18.16N), Lajas (67.08W, 18.03N), and Isabela (67.05W, 18.06N) could scan vertically or spatially, and were implemented only when western storms occurred.

All instruments were checked and calibrated before each phase. Researchers communicated daily to synchronize efforts. To ensure optimal radiosonde launch times, NWS forecasts and weather maps, along with aerosol optical thickness (AOT) forecasts from the NASA GEOS-5 model, were analyzed to ensure that a range of conditions including low and high AOT for dry and wet days were sampled. During Phase I, 12 radiosonde launches were carried out over a three week period. While Phases II and III were each a week shorter, they each had more launches than Phase I- an average of two-daily, during weekdays. Efforts were made to launch up to 30 min before forecasted storms and just after completion of afternoon/evening showers when possible during the two 2016 phases.

Conditions during CAST

Phase I (22 June–10 July 2015) was conducted during the extreme Caribbean summer drought of 2015, which occurred during a strong El Niño and a positive NAO phase. The drought caused island-wide emergency water management practices in Puerto Rico, including water rationing and potable water distribution. Precipitable water from the National Center for Environmental Prediction (NCEP) reanalysis dataset (and corroborated by satellite imagery) revealed negative anomalies in the Caribbean (3-4 kg m^{-2}, or 4-6% less than climatological averages), which along with cooler SSTs attained from the Optimum Interpolated Sea Surface Temperature (OISST) product (0.2–1 ^{0}C less than the 27.5 ^{0}C climatological value) could possibly mitigate rain production. Furthermore, frequent intense dust events occurred during

Phase I, and the regional 550 nm aerosol optical depth (AOD) average from the Moderate Resolution Imaging Spectroradiometer (MODIS) product was higher than usual, a value of 0.36 compared with the 14-year average value of 0.3 (2003-2016). In addition, ENSO was determined via the multivariate ENSO index (MEI) to be a warm event two standard deviations above normal; while drought strength determined from the Standard Precipitation Index (SPI) was three standard deviations below normal. These numbers are indicative of extremely dry Caribbean conditions, and are reflected in the reduced rain days over Puerto Rico, although maximum daily rain accumulations above 40 mm occurred over the island on 27% of Phase I campaign days. Precipitation anomalies from the Advanced Hydrologic Prediction Service (Fig. 3a) showed drier than normal conditions for more than 70% of the island in June by -25 mm or more, and for more than 85% of the island during July by -50 mm or more. Positive precipitation anomalies greater than 50 mm, however, occurred in June over the northwest quadrant, more than 20% of the island, and may be indicative of locally enhanced precipitation.

During the dry season (Phase II, 6-22 February 2016), positive precipitable water anomalies (8% , 38 kg m^{-2}) were found over western Puerto Rico and the Lesser Antilles, while negative anomalies (6%, 33 kg m^{-2}) were detected towards the central and southwestern of the Caribbean Sea. Despite SSTs near annual lows, values were warmer than February climatological values by 0.3-1 ^{0}C (26.5 ^{0}C seasonal average). Moreover, dust content was low with an AOD average of 0.19, normal for February. Locally over Puerto Rico, rain exceeding 40 mm fell on 70% of days, with positive rainfall anomalies above 50 mm in the northwest and in pockets along the west, southeast and south-central coasts, and El Yunque (Fig. 3b).

Early rainfall season (Phase III, 24 April–7 May 2016) SSTs were unseasonably high by 0.4-1.0 ^{0}C, approximately 28 ^{0}C in the Caribbean Sea. Furthermore, precipitable water anomalies of 6-10% (42-44 kg m^{-2}) were detected along with lower than usual AOD, 0.23 as compared with the 0.26 14-year MODIS average. Positive April rainfall anomalies above 50 mm in Puerto Rico occurred along all but the western coasts (Fig. 3c), with negative anomalies of 50-100 mm along the Cordillera mountain range. However, trends changed during May with negative precipitation anomalies exceeding 50 mm at the center, southern coast, and northeast quadrant. Phase III was the wettest of the three, with maximum rain totals above 40 mm on 71% of days, an expected result considering the warmer SSTs, positive precipitable water anomalies, and low dust during the period.

CAST Data

The ceilometer 910 nm backscatter aerosol signature varies diurnally and seasonally (Fig. 4), showing maximum intensity between the surface and 4 km during Phase I, and decreased intensity during Phases II and III most notably between the surface and 0.5 km. Column integrated AOT from AERONET (not shown) yields 1640 nm average large-particle AOT values of 0.256, 0.066, and 0.074 for Phases I to III respectively, while 500 nm (medium particle) values are 0.342, 0.107, and 0.130 respectively, and 340 nm (small particle) averages are 0.348, 0.123, and 0.250 respectively, exhibiting a nearly four-fold increase in large wavelength (large particle) AOT comparing Phase I to II-III. Soil moisture 0.2 m below the surface, maximum precipitation, and 500 nm AOT for each phase is presented in Figs. 5a-5c. Phases I-II show wetter soil conditions at western sites (Cabo Rojo, Maricao, and Guillarte) than further east (Corozal 66.36W, 18.32N), while soil moisture in the east increases in Phase III.

Composites of all the radiosonde launches for each phase (Figs. 5d-5f) show higher CAPE during Phases I and III than during Phase II. Lower wind speeds (at levels >700 mb) are observed during Phase I (Fig. 5d) as compared with Phases II and III (Figs. 5e and 5f). Local precipitable water in Phases I and III are higher than in Phase II by an average of approximately 0.01 m. The dry season (Phase II) also exhibits the lowest convective inhibition values (CIN) of all three phases, and mixing heights (0-1.5 km) between the minimums produced in Phase I (0-1 km) and the maximums produced in Phase III (0-2 km). Dew point depressions (not shown) between 800 and 400 mb were highest (>50^{0}C) during non-rain Phase II days, as compared to Phases I and III, with averages of 35 and 20^{0}C, respectively. In the following section, we focus on one CAST event via presentation of the campaign data.

A CAST case study

To illustrate the value of CAST data, we present a large storm that took place over western Puerto Rico on 18 February 2016 as a case study. The rain event occurred as a mid to upper level ridge eroded, and a polar trough shifted into the Central Atlantic. The intense rainfall yielded rain accumulations of 50 mm or more in a period of 12 hours, mostly over the northwestern and western slopes of the Cordillera Central (Fig. 6a). Ceilometer data (Fig. 6b) shows moderate backscatter intensity prior to the beginning of the rainfall at UPRM (1845 AST), and cloud heights ranging from as low as 0.5 km to beyond 4 km (instrument detection limit is 4.5 km). A Skew-T diagram of the 1251 and 1648 radiosonde launches (Fig. 6c) show cloud levels as high as 600 mb, land surface temperatures at ~28 ^{o}C, and evidence of westerly sea-breeze strengthening from the early to late afternoon hours. In addition, the environment became more humid from the early to late afternoon. AERONET 500 nm AOT (Fig. 6d) at La Parguera and UPRM ranged from 0.11 to 0.25, high compared to the Phase II average (0.107). Soil moisture at the Cabo Rojo site (also Fig. 6d) was nearly constant until 1745 AST, when it increased 5-13 points from the surface to the 0.5 m depth in response to the rainfall.

CAST data points at the very least to localized enhancement of this rain event due to topography and strong sea-breeze influence (revisiting the convection process diagram of Fig. 1), although further study is necessary to determine the individual contributions of these factors in convection enhancement, and their interplay with the leading large-scale conditions.

Closing remarks

CAST observations have provided pertinent information about atmospheric conditions in western Puerto Rico during three of the island's distinct seasons, providing a starting point for the analysis of convective interplay in the coastal tropics. The results reported herein are only a first step in furthering our understanding of the interconnectedness of multi-scale precipitation drivers in tropical coastal environments to support the overall long-term goal of improving weather prediction in sensitive and complex regions such as the Caribbean.

Future CAST phases will allow for additional cross-seasonal comparisons and analysis. CAST also provides a basis for setting up modeling experiments centered around some of the more extreme convective events occurring during the experiment. The incorporation of a cloud resolving model will allow us to further investigate multi-scale interactions between large and local scale processes and zoom in on their effects on island convection and precipitation. CAST data, event descriptions, and synthesis reports to date may be accessed at the CCNY Coastal Urban Environmental Research Group website (http://cuerg.ccny.cuny.edu/).

Acknowledgements

Thhanks to NSFAGS-1433430, DOEd #P031M105066, and NOAA-CREST (NA17AE1625) for their support and AERONET, NRCS, NCEP, and NOAA for data used herein. Special thanks to V. Morris, W. Peña, C. Lunger, J. Diaz, D. Gonzalez, and R. Davis.

For further reading

Angeles, M. E., J. E. González, N. D. Ramírez-Beltrán, C. A. Tepley, and D. E., Comarazamy, 2010: Origins of the Caribbean rainfall bimodal behavior, *J. Geophys. Res.*, **115**, D11106, doi:10.1029/2009JD012990.

Carlson, T. N., and J. M. Prospero, 1972: The large-scale movement of Saharan air outbreaks over the Northern Equatorial Atlantic, *J. Appl. Meteor.*, **11**, 283–297, doi: 10.1175/1520-0450(1972)011<0283:TLSMOS>2.0.CO;2.

Gamble, D. W., and S. Curtis, 2008: Caribbean precipitation: Review, model, and prospects, *Prog. Phys. Geog.*, **32**, 265–276, doi: 10.1177/0309133308096027.

Hosannah, N., H. Parsiani, and J. E. González, 2015: The role of aerosols in convective processes during the midsummer drought in the Caribbean, *Adv. in Meteor.*, **2015**, doi:10.1155/2015/261239.

Jury, M. R., S. Chiao, and E. W. Harmsen, 2009: Mesoscale structure of trade wind convection over Puerto Rico: Composite observations and numerical simulation, *Boundary-Layer Meteor.*, **132**, 289-314, doi:10.1007/s10546-009-9393-3.

Keyantash, J. and J.A. Dracup, 2002: The quantification of drought: An evaluation of drought indices. *Bull. Amer. Meteor. Soc.*, **83**, 1167-1180, doi: 10.1175/1520-0477(2002)083<1191:TQODAE>2.3.CO;2.

Rosenfeld, D., Y. Rudich, and R. Lahav, 2001: Desert dust suppressing precipitation: A possible desertification feedback loop, *PNAS*, **98**, 5975-5980. doi:10.1073/pnas.101122798.

Wolter, K., and M. S. Timlin, 2011: El Niño/Southern Oscillation behaviour since 1871 as diagnosed in an extended multivariate ENSO index (MEI.ext)., *Intl. J. Climatol.*, **31**, 1074-1087, doi: 10.1002/joc.2336.

Figure Captions List

Figure 1. Topographic map of Puerto Rico (m, shaded) showing local processes including surface heating, orography (red-white and blue-white arrows lifting up mountains), and convergence between sea-breeze (red arrows) and easterly (blue arrows) winds. Sensor sites are also shown, including the NWS NEXRAD radar site (NEX), Tropinet radar sites (purple dots) and ranges (purple dashes), UPRM site (UPRM), La Parguera site (LP), San Juan (SJ), NRCS soil moisture sites (black dots), and the Cabo Rojo soil moisture site (silver dot).

Figure 2. Instruments and field study preparation: a) Cabo Rojo Tropinet radar system, b) preparing radiosonde balloon, c) radiosonde atop UPRM building, d) readying Mayaguez site ready for soil moisture sensors, and e) soil moisture sensor.

Figure 3. Advanced Hydrologic Prediction Service (AHPS) total precipitation monthly climatological anomalies (mm) and prevailing background flow direction for CAST Phases: a) I, b) II, and c) III.

Figure 4. Ceilometer 910 nm backscatter for CAST Phases I (black rectangle), II (orange rectangle), and III (red rectangle).

Figure 5. AHPS Normalized Maximum precipitation (blue line), 500 nm AERONET AOT (red line), and 0.2 m depth soil moisture for NRCS Maricao (aqua bars), Guillarte (orange bars), Corozal (light blue bars), and CAST Cabo Rojo (brown bars) during CAST Phases: a) I, b) II, and c) III. And radiosonde data for Phase I: d) horizontal wind (barbs), CAPE (J kg^{-1}, black line), CIN (red line), precipitable water (orange line), and mixing height (pink line), same for Phases II (e) and III (f).

Figure 6. Data for the 18 February 2016 storm. a) AHPS total accumulated precipitation, b) CL51 backscatter intensity, c) radiosonde data (left are dew point temperature plots, right are ambient temperature) at 1251 (red lines) and 1648 (blue lines) AST, and d) Cabo Rojo soil moisture content and 500 nm AERONET AOT at UPRM and La Parguera.

Tables

Table 1: CAST phase log.

Phase	Days with max rain >40 mm	Days with sea breeze	Background flow	Days with Orographic effects	Days with AOT (1020 nm) > 0.2	1300 AST Relative humidity
I *6/22/15 – 7/10/15*	5/19	9/19	E to ENE	4/19	12/19	75 to 88
II *2/6/16 – 2/22/16*	12/17	8/17	S to NNE	6/17	0/17	52 to 89
III *4/24/16 – 5/7/16*	10/14	1/14	S to ENE	2/14	2/14	73 to 90

Figures

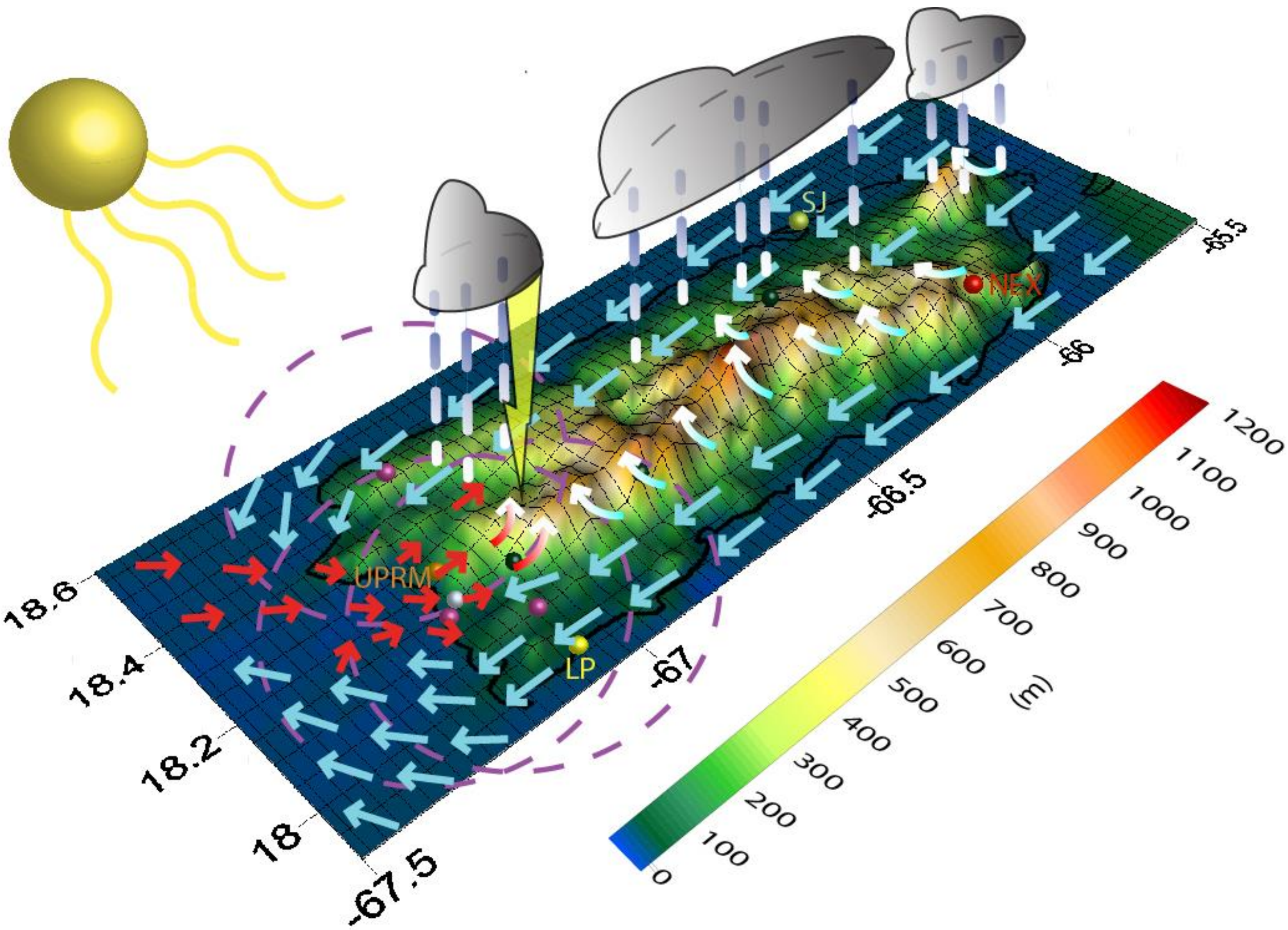

Figure 1. Topographic map of Puerto Rico (m, shaded) showing local processes including surface heating, orography (red-white and blue-white arrows lifting up mountains), and convergence between sea-breeze (red arrows) and easterly (blue arrows) winds. Sensor sites are also shown, including the NWS NEXRAD radar site (NEX), Tropinet radar sites (purple dots) and ranges (purple dashes), UPRM site (UPRM), La Parguera site (LP), San Juan (SJ), NRCS soil moisture sites (black dots), and the Cabo Rojo soil moisture site (silver dot).

Figure 2. Instruments and field study preparation: a) Cabo Rojo Tropinet radar system, b) preparing radiosonde balloon, c) radiosonde atop UPRM building, d) readying Mayaguez site ready for soil moisture sensors, and e) soil moisture sensor.

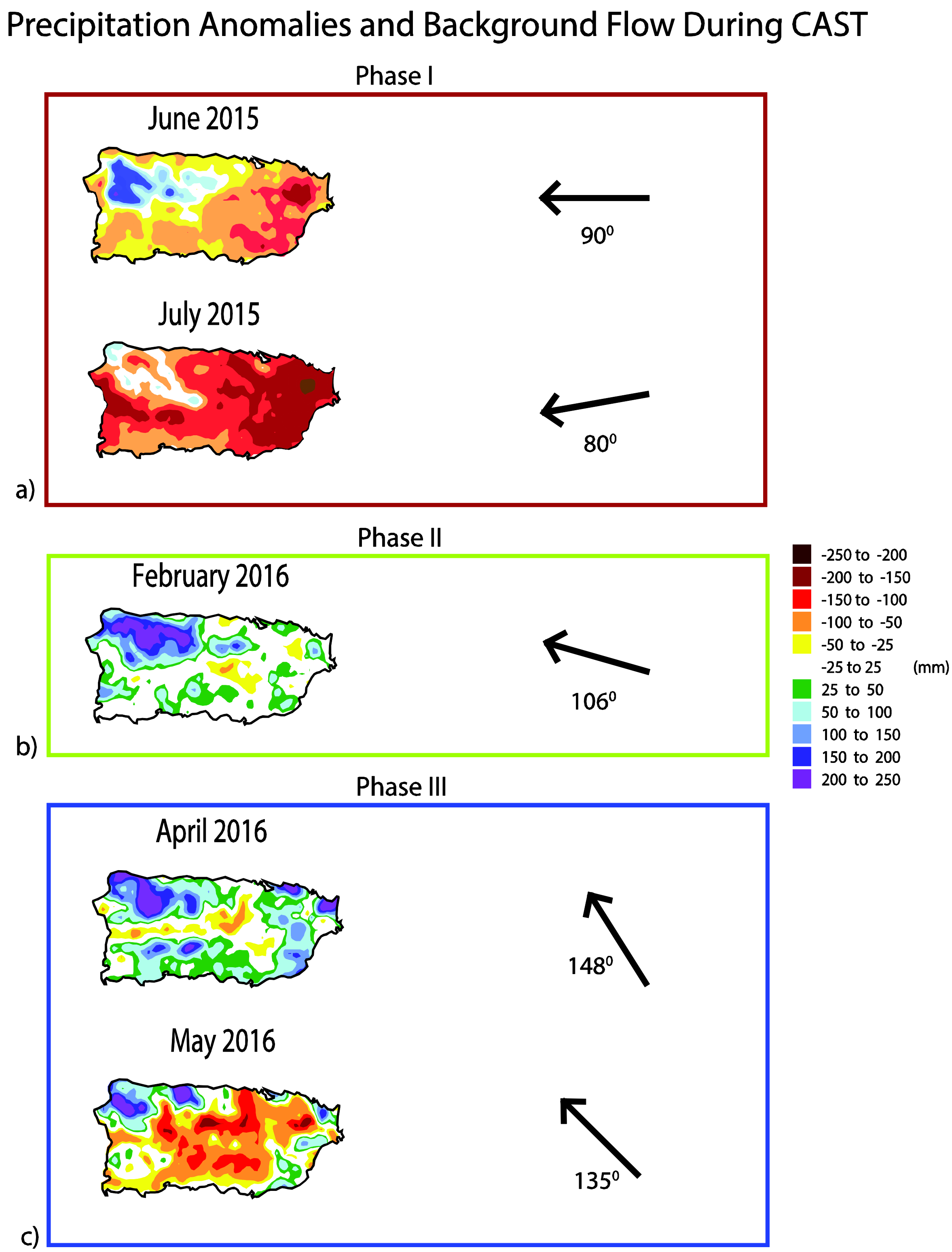

Figure 3. Advanced Hydrologic Prediction Service (AHPS) total precipitation monthly climatological anomalies (mm) and prevailing background flow direction for CAST Phases: a) I, b) II, and c) III.

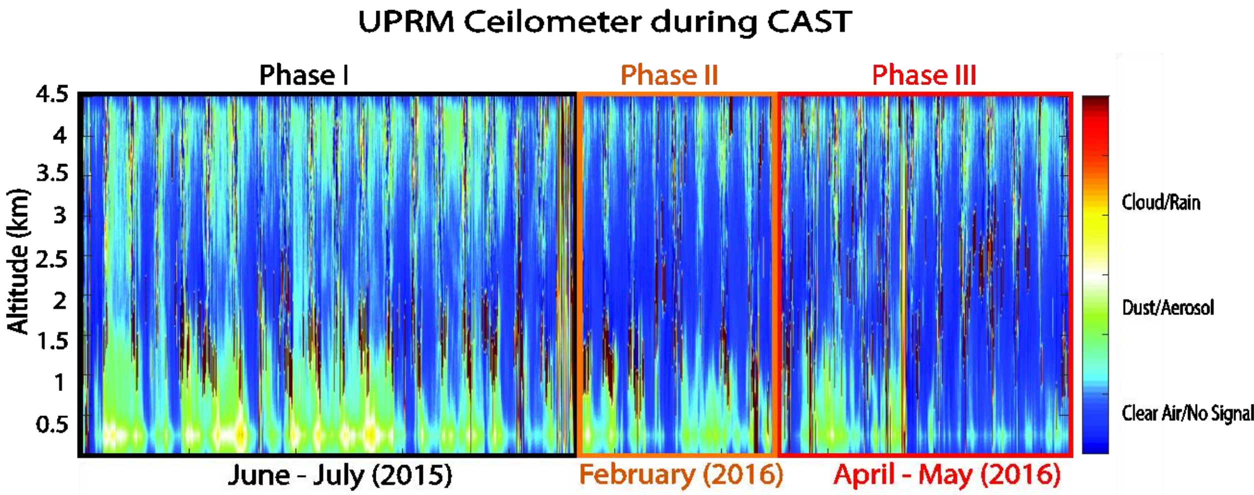

Figure 4. Ceilometer 910 nm backscatter for CAST Phases I (black rectangle), II (orange rectangle), and III (red rectangle).

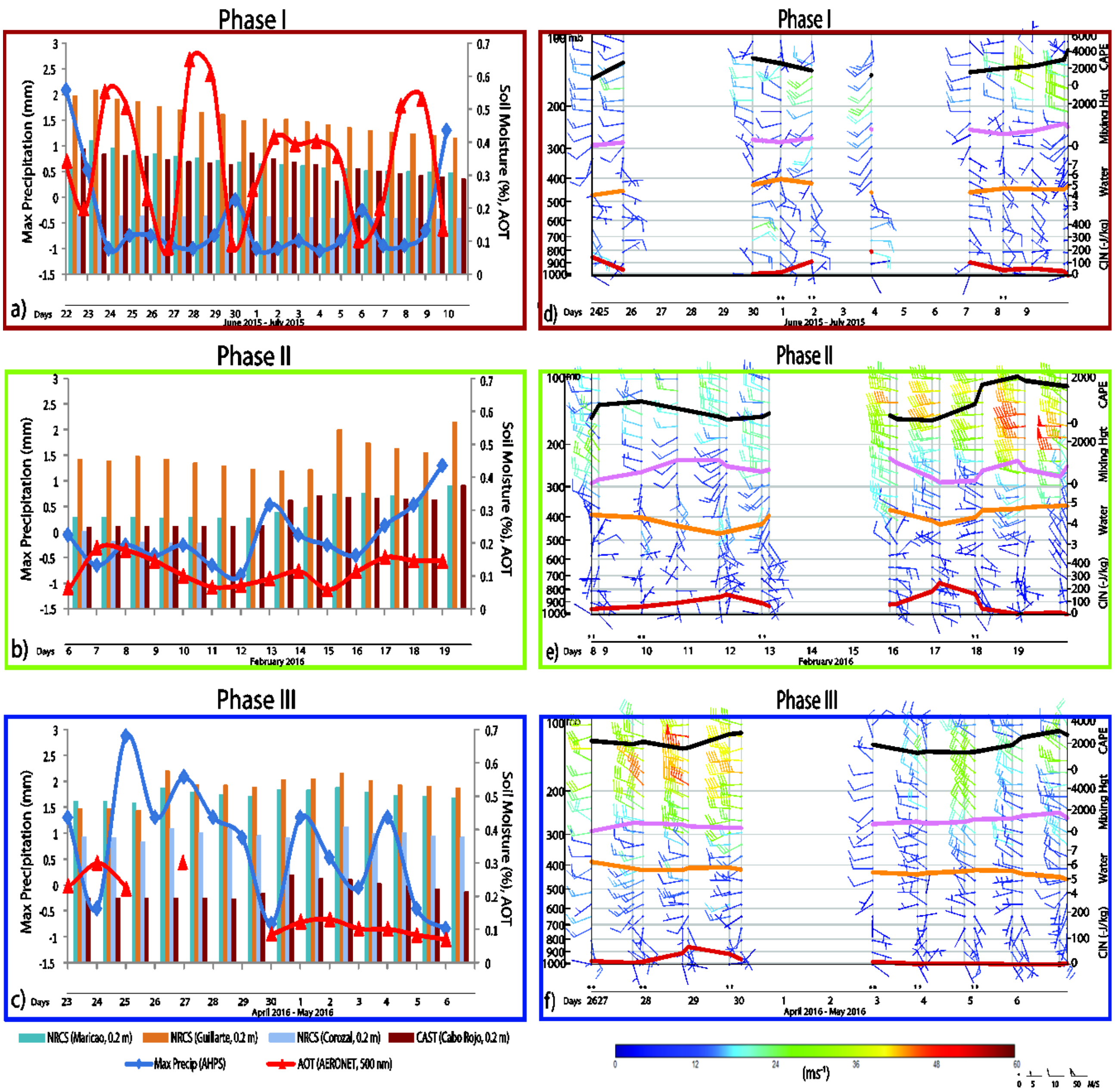

Figure 5. AHPS Normalized Maximum precipitation (blue line), 500 nm AERONET AOT (red line), and 0.2 m depth soil moisture for NRCS Maricao (aqua bars), Guillarte (orange bars), Corozal (light blue bars), and CAST Cabo Rojo (brown bars) during CAST Phases: a) I, b) II, and c) III. And radiosonde data for Phase I: d) horizontal wind (barbs), CAPE (J kg^{-1}, black line), CIN (red line), precipitable water (orange line), and mixing height (pink line), same for Phases II (e) and III (f).

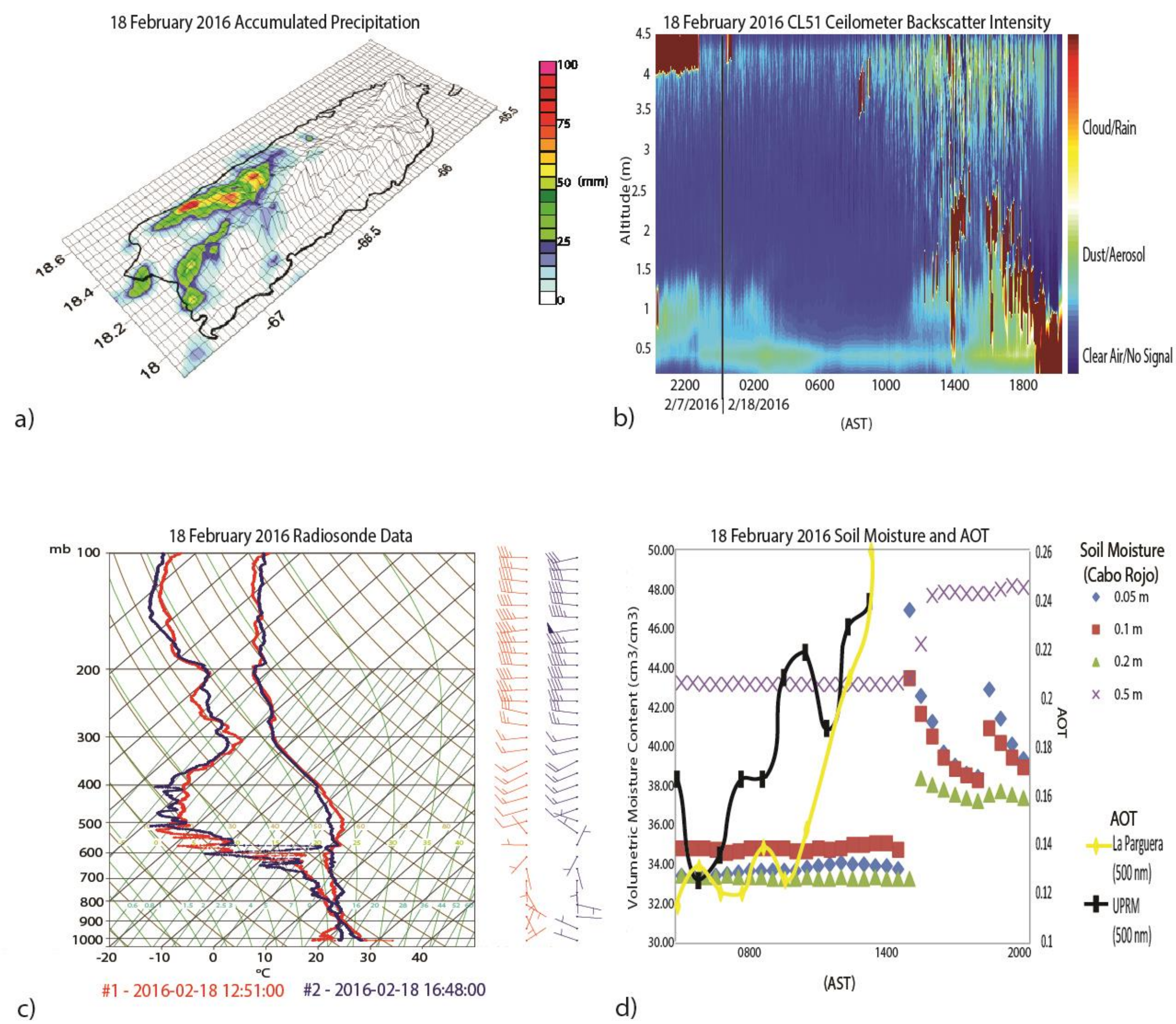

Figure 6. Data for the 18 February 2016 storm. a) AHPS total accumulated precipitation, b) CL51 backscatter intensity, c) radiosonde data (left are dew point temperature plots, right are ambient temperature) at 1251 (red lines) and 1648 (blue lines) AST, and d) Cabo Rojo soil moisture content and 500 nm AERONET AOT at UPRM and La Parguera.